IEEE Access
Multidisciplinary | Rapid Review | Open Access Journal

Received 27 October 2023, accepted 28 November 2023, date of publication 30 November 2023,
date of current version 8 December 2023.

Digital Object Identifier 10.1109/ACCESS.2023.3338552

RESEARCH ARTICLE

Mechanistic Study of a Low Frequency Piezoelectric Motor With Natural Frequency Adjustment Method

XIAOTAO LI[1], SHENGJIANG WANG[1], XIANGYOU PENG[1], GUAN XU[2], (Member, IEEE), JINGSHI DONG[1], AND FENGJUN TIAN[1]

[1]School of Mechanical and Aerospace Engineering, Jilin University, Nanling Campus, Changchun, Jilin 130025, China
[2]Transportation College, Jilin University, Nanling Campus, Changchun, Jilin 130025, China

Corresponding author: Guan Xu (xuguan@jlu.edu.cn)

This work was supported in part by the National Natural Science Foundation of China under Grant 52005214, and in part by the Science and Technology Research Project of the Education Department of Jilin Province under Grant JJKH20220986KJ.

ABSTRACT A variable frequency piezoelectric motor is studied, which can generate rotational motion under the excitation of variable-mode vibration response units. Two variable-mode vibration response units fixed in the inclined plane are excited by the square wave and drive the friction disk to achieve the rotation and translation. Thus, the friction torque on the rotor changes periodically, and the rotor is driven to produce positive displacement output. By adjusting the mass distribution of the variable-mode piezoelectric wafer vibration response unit, the natural frequency of the low-frequency motor is adjustable. In order to achieve the maximum displacement output of the low-frequency motor, the simulation analysis is initially performed on the stiffness, mode, and vibration shape in line with the motion principle. Then the experiments of the variable-natural-frequency motion characteristics of the low frequency motor are carried out, and the maximum rotation speed of the designed piezoelectric motor is improved by the variable-natural-frequency motion characteristics and reaches 520 mrad/s.

INDEX TERMS Piezoelectric motor, variable-natural-frequency, mass distribution.

I. INTRODUCTION

Piezoelectric motor is a modern type of actuator that uses piezoelectric drive element as a vibration excitation and employs the friction effect to actuate the rotor. In the field of precision actuation, piezoelectric actuators play an important role in micro electro mechanical systems (MEMS), micro and nano positioning [1], [2], energy acquisition [3], [4], [5], aerospace [6], optical scanning [7], [8], [9], biomedical engineering [10], [11], [12], and 3D printing [13] etc.

Piezoelectric motor, as a type of piezoelectric actuator, taking the advantages of small volume, high torque output, flexible structure, no electromagnetic disturbance, fast response, and low cost [14], [15], etc. Thus, the researchers are attracted by the piezoelectric motor studies. Mukhopadhyay et al. [16] proposed a piezoelectric ultrasonic motor for haptic system applications with an ultrasonic actuator with a maximum output force of 1.6 N at 50 V and an optimum output force of 1 Jūrėnas et al. [17] introduced a new three-degree-of-freedom piezoelectric ultrasonic motor with a spherical rotor, its speed is 30 r/min at the operation frequency of 92 kHz. Borodinas et al. [18] presented a harmonic single-phase signal-driven piezoelectric motor which utilizes the radial vibration shape of the symmetrical coplanar piezo structure and three contact points. It achieved the rotation movement with a resonant frequency of about 91.3 kHz. Bansevicius et al. [19] developed a design with two active motion pairs for the piezoelectric cylindrical actuator. The speed is 4.05×10^{-4} r/min under the working frequency of 93.6 kHz. Zhang et al. [20] studied a two-degree-of-freedom rotation motor, which adopts two layers of four orthogonal piezoelectric wafers. The rotation speed about X axis is 263.26 mrad/s and the rotation speed about Y axis is 268.48 mrad/s. Wang et al. [21] explored the centrally

The associate editor coordinating the review of this manuscript and approving it for publication was Shuo Sun.

symmetric flexible hinge mechanism for the rotary piezoelectric actuator. The rotor is driven by the piezoelectric stack in the center of the two rings structure. The rotation speed of the rotary actuator is 55 mrad/s under the driving frequency of 600 Hz. Wang et al. [22] designed a rotary compact-structure positioner. Two piezoelectric stacks are used to drive the four feet, which rotate the center rotor. The speed of the positioner is 151.4 mrad/s under the frequency of 700 Hz.

Most of the currently available piezoelectric motors operate in the high-frequency range. However, operation at high frequencies affects the stability of the motion and also accelerates the abrasion of the contacting surfaces. Liang et al. [23] proposed a rotary piezoelectric motor with two orthogonal piezoelectric stacks based on friction and harmonic actuation method, which drives the rotor rotation by friction with the excitation frequency of 5 Hz. Xing and Qin [24] proposed a novel magnetic field modulated piezoelectric motor. The drive system combines a piezoelectric drive with magnetic modulation to convert the reciprocating oscillation of the stator into stepping operation of the rotor. The drive frequency is 3 Hz and the desirable speed output is 1.74 mrad/s. Wang et al. [25] proposed a low frequency motor actuated by a sinusoidal signal. It consists of a status part and a rotor part. The status part has an asymmetrical design, which produces torsional vibration while actuated by a single-phase sinusoidal signal. The working frequency used is 50 Hz and the maximum angular velocity is 450.29 mrad/s. Zhang et al. [26] presented a dual-degree-of-freedom pointing mechanism adopting a bending-bending hybrid piezoelectric actuator. The mechanism is based on the principle of inertial drive, and the rotational motion around two rotation axes is realized by an actuator. The maximum rotation speeds of the rotor around the two axes are 153 mrad/s and 154 mrad/s, respectively.

Piezoelectric motors within the low-frequency range have the advantages of low vibration noise and low wear However, none of the above motors can adjust the natural frequency of the motor. The purpose of variable frequency regulation is to effectively avoid resonance and prevent rapid damage to the motor by adjusting the natural frequency of the motor, when the frequency of the working signal is constant. In addition, the natural frequency of the motor is adjustable to be close to the working frequency, which increases the vibration of the wafer, provides greater driving inertia force and improves the driving ability. For example, a precision positioning workbench is a vibration system with external loads. The natural frequency of the vibration system changes with the different external load. Thus, it is necessary to adjust the natural frequency of the piezoelectric motor system to avoid resonance frequency and work in the quasi-resonant range for the optimal driving capability. Therefore, the paper proposes a piezoelectric low frequency motor and realizes variable modal performance for the piezoelectric low frequency motor. A motion mechanism of piezoelectric low-frequency motor under the excitation of variable-mode vibration response unit is presented. The variable-mode vibration response unit is analyzed and optimized for its structure design. The frequency response characteristics are simulated and experimentally analyzed to realize variable-frequency adjustment of the piezoelectric motor and the motion characteristics are improved by the variable-natural-frequency motion characteristics.

II. METHOD AND SIMULATION OF VARIABLE-NATURAL-FREQUENCY VIBRATION UNIT OF MOTOR

A. METHOD OF VARIABLE-NATURAL-FREQUENCY VIBRATION UNIT OF MOTOR

As a key driving element of a piezoelectric low frequency motor, the frequency adjustment characteristics of a variable-mode piezoelectric wafer vibration response unit are essential to the mechanism of a variable-natural-frequency low frequency motor. Therefore, a variable-mode piezoelectric wafer vibration response unit is proposed as shown in Fig. 1, including a piezoelectric wafer, a variable-natural-frequency substrate, a mass block and a clamping piece. The variable-natural-frequency substrate, the mass block, and the substrate in piezoelectric wafer are made by brass with the Young's modulus of 99.95 GPa, and the Poisson's ratio of 0.34. Piezoelectric material is pzt51 with the Poisson's ratio of 0.34 and the Young's modulus of 66 GPa. The overall size of the vibration response unit is 134 mm×33 mm×7 mm. The variable frequency substrate takes three circular holes, which are located at 1-3 positions from the clamping piece to the wafer. The mass block is bolted to the variable-natural-frequency substrate, and the frequency adjustment of the variable-mode piezoelectric wafer vibration response unit is realized by altering the mass block position with respect to the clamping piece. When the relative mass block position to the clamping piece of the variable-mode piezoelectric wafer vibration response unit is changed, the natural-frequency as well as the vibration feature of the variable-mode piezoelectric wafer vibration response unit will be changed. Therefore, the natural-frequency and vibration mode of the variable-mode piezoelectric wafer vibration response unit are analyzed by altering the relative position of the mass block to the clamping end.

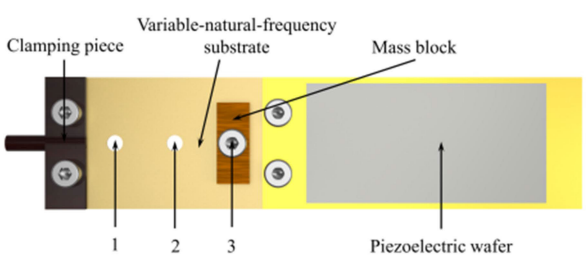

FIGURE 1. Vibration response unit of variable-mode piezoelectric wafer.

B. FREQUENCY SIMULATION ANALYSIS OF VARIABLE NATURAL-FREQUENCY VIBRATION UNIT OF MOTOR

As the natural-frequency is influenced by the stiffness, the simulation focuses on the stiffness of vibration unit. The stiffness of the variable-mode piezoelectric wafer vibration response unit can be adjusted by changing the mass block position of the variable-frequency substrate. Thus, the variable-mode piezoelectric wafer vibration response unit is subjected to finite element analysis to solve for the natural-frequency of the variable-mode piezoelectric wafer vibration response unit when the mass block is located at different positions of the substrate. The piezoelectric material is pzt-5H. The mass block is made of copper. The clamping block is made of hard aluminum. The handle of the clamping piece at the left end is fixed in the simulation. A static force, 1 N is added to the lower face of the substrate, and the model is meshed to solve the frequency adjustment part of the variable-mode piezoelectric wafer vibration response unit. The results are shown in Fig. 2. It can be seen that the maximum deflection of the end of the substrate is 0.949 mm, 1.163 mm, and 1.313 mm for the mass block at position 1, 2, and 3, respectively. The stiffness at the three positions can be calculated as $k_1 = 1053.74$ N/mm, $k_2 = 859.85$ N/mm, $k_3 = 761.61$ N/mm. It can be seen that the greater the distance of the mass block from the fixed position is, the lower its stiffness is.

In order to further analyze the response characteristics of the variable-mode piezoelectric wafer vibration response unit by changing the relative position of the mass block, the natural frequency of the variable frequency substrate is studied by [27]

$$\omega_n = (3EI/ml^3)^{1/2} \tag{1}$$

where m is the mass of the mass block, E is the elastic modulus, I is the moment of inertia, and l is the distance from the mass block to the fixed end. It can be seen that the stiffness and mass distance are the key parameters of the natural frequency of the substrate under the condition of the same mass. From (1), the stiffness of the variable frequency substrate is related to the distance of the mass block from the fixed end. The greater the distance is, the lower its stiffness is and the lower the natural frequency of the variable frequency substrate is.

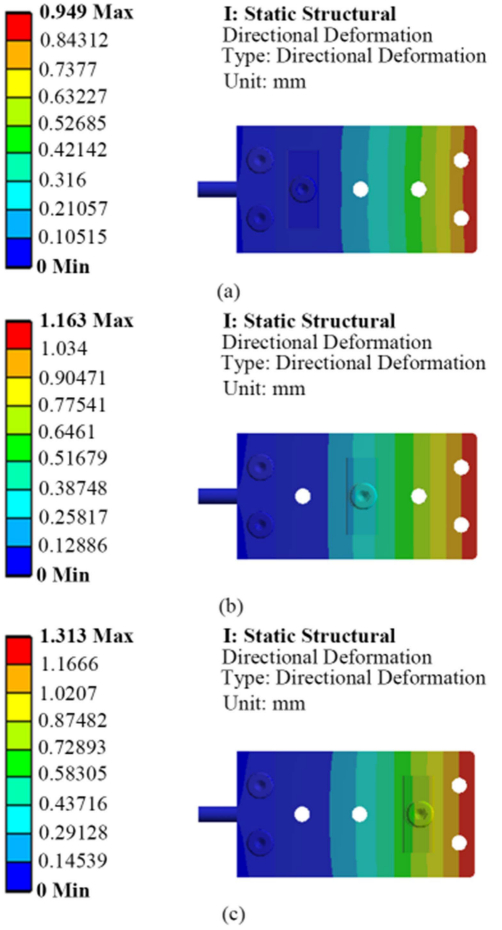

FIGURE 2. Stiffness analysis of variable natural-frequency substrate. (a) Position 1. (b) Position 2. (c) Position 3.

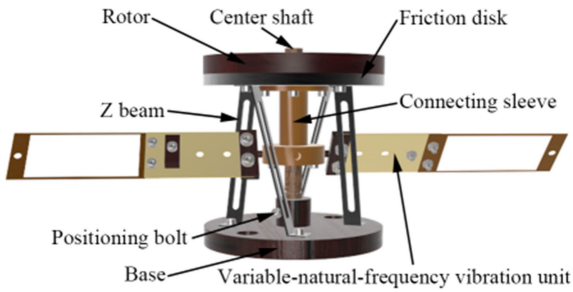

FIGURE 3. Structure of piezoelectric variable-natural-frequency motor.

III. METHOD AND MOTION PRINCIPLE ANALYSIS OF LOW VARIABLE-NATURAL-FREQUENCY MOTOR

A. METHOD OF LOW VARIABLE-NATURAL-FREQUENCY MOTOR

The 3D model of the piezoelectric low frequency motor is designed in Fig. 3. The basic components of the piezoelectric low frequency motor are a rotor, a friction disk, two variable-natural-frequency vibration units, four Z beams, a base, a connecting sleeve, a center shaft, and a positioning bolt. The base, the Z beam, the center shaft, the rotor, the friction disk, the connecting sleeve and the clamping piece are made by hard aluminum with the Young's modulus of 71 GPa, and the Poisson's ratio of 0.33. The overall size of the motor without the vibration response units is φ100 mm$\times$108 mm. The driving element is the variable-natural-frequency vibration unit, whose angle about the bottom surface can be adjusted by the clamping piece. There are two variable natural-frequency vibration units, which are fixed at the lower end of the connecting sleeve. The base is fixed on the anti-vibration table, and the Z beam is used to connect the base with the friction disk. The friction disk and the rotor have holes in the center. The rotor is connected to the center shaft by a bearing, and its

lower surface has a clearance with the friction disk. The center shaft can be adjusted along the shaft axis with the clearance of the rotor and friction disk, and fixed to the base with the positioning bolt. The pre-pressure between the rotor and friction disk is adjusted by the thread between the base and the center shaft. The low frequency motor adopts the alternating force from the variable-natural-frequency vibration unit, to rotate the rotor by the friction force periodically.

B. MOTION PRINCIPLE OF LOW VARIABLE-NATURAL-FREQUENCY MOTOR

Due to the rapid change of the square wave excitation signal, the mass block can generate greater inertial force for the faster driving speed. Therefore, the study adopts the square wave as the excitation signal. Piezoelectric low-frequency motor adopts a square wave excitation signal. The motion principle of the low-frequency motor is explained with two opposite variable-mode piezoelectric wafer vibration response units. According to the same excitation signal for the variable-natural-frequency piezoelectric wafer response units, the driving process in Fig. 4 of the piezoelectric motor can be divided into the following steps. Fig. 4a shows the excitation signal, and Fig. 4b shows the motor state without the excitation signal input.

(1) The excitation signal is turned on. For the voltage of U_2, the motor status is shown in Fig. 4c. The piezoelectric wafer is tilted downwards, and the motor is in the holding stage. The positions of the rotor and friction plate are marked by red and yellow lines. At the moment t_0, the external excitation increases from U_0 to U_1. The variable-natural-frequency vibration unit generates the oblique upward inertial force in Fig. 4d, which is decomposed to the vertical force F_z and the counterclockwise tangential force F_{xy}. The vertical force F_z stretches the Z beam, causing an increase in the pressure between the friction disk and the rotor. The tangential force F_{xy} causes the friction disk to rotate counterclockwise. The rotor rotates θ_1 together with the friction disk under the action of frictional torque.

(2) From t_0 to t_1, the voltage is U_1, and the motor state is shown in Fig. 4e. The piezoelectric wafer is tilted upwards, and the motor is in the holding stage.

(3) At the moment t_1, the external excitation changes from U_1 to U_2, and the variable-natural-frequency vibration units instantly generates an oblique downward inertial force. This inertial force can be decomposed into a vertical downward component force F'_z and a tangential force F'_{xy} in a clockwise direction along the circumference. F'_z causes the Z beam to contract downward, reducing the positive pressure between the friction disk and the rotor, while F'_{xy} causes the friction disk to rotate clockwise. The rotor rotates θ_2 together with the friction disk under the action of frictional torque.

(4) From t_1 to t_2, the voltage is U_2, and the motor returns to the state shown in Fig. 4c. One cycle of movement of the motor is achieved. The total displacement of the rotor in a period is $\theta = \theta_1\text{-}\theta_2$.

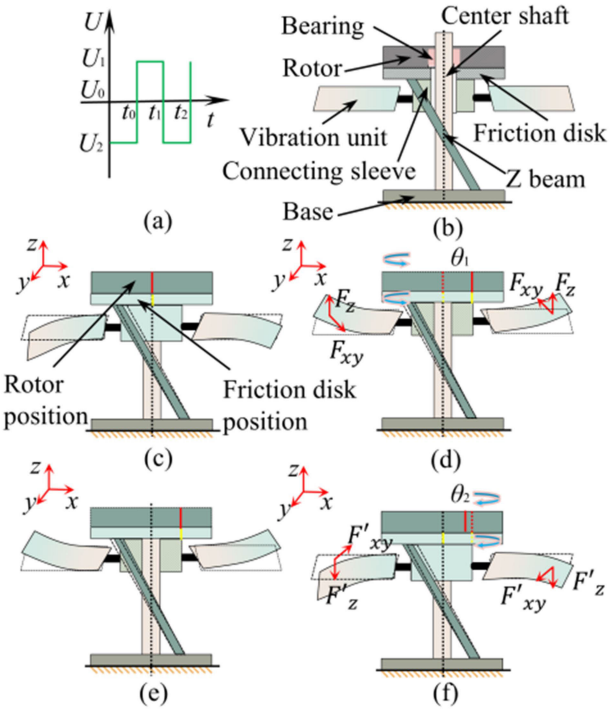

FIGURE 4. Motion principle of piezoelectric variable-natural-frequency motor. (a) Excitation signal. (b) Motor structure. (c) Initial state. (d) t_0. (e) $t_0 \sim t_1$. (f) t_1.

C. SIMULATION ANALYSIS OF LOW VARIABLE-NATURAL-FREQUENCY MOTOR

Before the experimental testing on the piezoelectric motor, the vibration mode simulation analysis is carried out for the mass block at position 3, which is beneficial for initially selecting the suitable vibration mode and driving frequency ranges. The boundary condition is the fixed bottom surface of the base. The connection relationship among the motor parts is *bonded*, and 1 mm is chosen for meshing. The vibration mode simulation results are shown in Fig. 5. The first six modes and natural frequencies of the piezoelectric motor are simulated and analyzed. The natural frequencies are 19.251 Hz, 19.499 Hz, 68.978 Hz, 79.789 Hz, 89.356 Hz, and 93.613 Hz, respectively. It can be seen that the first six natural frequencies are all in a lower range. A reasonable vibration mode is essential for the motor, which can improve the driving performance. For the first and second order modes, it can be seen that only the vibration unit is in the motion state, while there are rarely the rotation and up-down vibration of the friction plate. Moreover, the vibration of the second order of the vibration unit is asymmetric, which contradicts the motion principle. Thus, the first and second order modes are not chosen. For the fourth and fifth order modes, it can be seen that the friction disk generates large translational amplitude in the horizontal plane, while there is rarely the rotation of the friction disk. As the fourth and fifth orders also contradict the motion principle, they are not chosen. For the third order vibration mode, the rotation of the friction disk and the linear

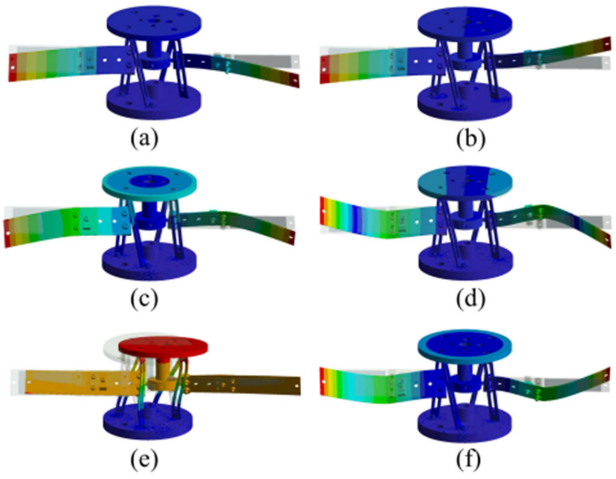

FIGURE 5. Vibration modes of variable-natural-frequency motor for the mass block at position 3. (a)-(f) first–sixth order modes.

motion along the vertical direction are larger compared with the ones of the sixth order mode. Therefore, the third order mode is chosen on the basis of the motion principle.

According to the modal analysis on the variable-natural-frequency motor at position 3, the modal analysis is further conducted on position 1, 2, and 3. The third-order mode shapes and natural frequencies are shown in Fig. 6. The natural frequencies are 72.808, 70.734, and 68.978 Hz. respectively. As the mass block moves from position 1 to position 3, the natural frequency of the variable-natural-frequency motor gradually decreases. It indicates the feasibility of variable natural frequency of the piezoelectric motor by changing the mass block position.

IV. EXPERIMENTAL TESTING AND ANALYSIS OF LOW VARIABLE-NATURAL-FREQUENCY MOTOR

A. EXPERIMENT CONFIGURATION

According to the principle analysis and simulation of the low variable-natural-frequency motor, the experimental system of the variable-natural-frequency motor is established in Fig. 7, in order to test the driving performance of the motor. The experimental system includes a function generator, DG4062, Rigol Technology Inc., a power amplifier, RH41-D, Harbin Rongzhi Naxin Technology Co. Ltd., a laser micrometer, LK-H020, Keyence, a vice, a variable-natural-frequency motor prototype, and a data acquisition computer.

The frequency sweep experiment of the variable-mode piezoelectric wafer vibration response unit and the variable-natural-frequency motor without the rotor is carried out in the range of 0-400Hz. The resonant frequency regions of the variable-mode piezoelectric wafer vibration response unit and the variable-natural-frequency motor are identified at different positions of the mass block, which explore the effect of the mass block position on the natural frequency of the variable-mode piezoelectric wafer vibration response unit and the motor. Moreover, a driving performance analysis of

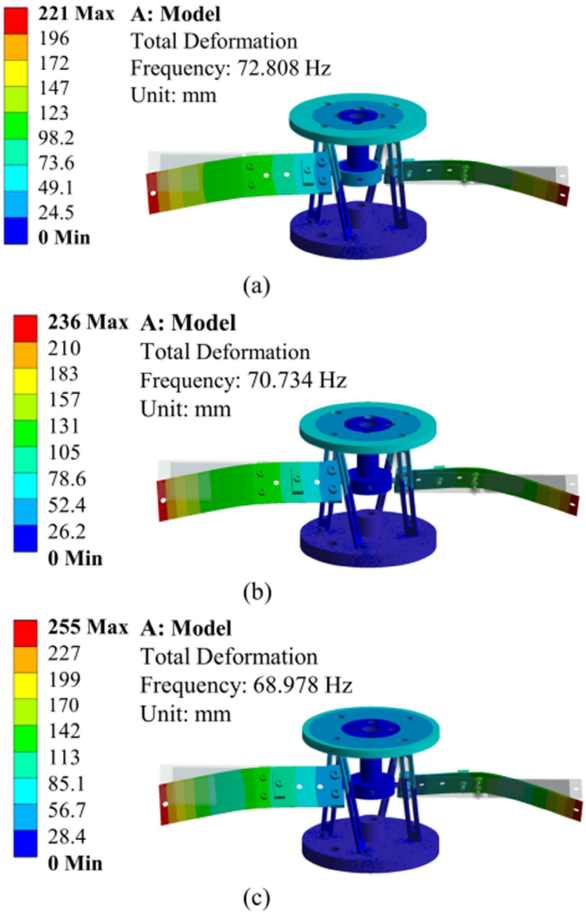

FIGURE 6. Simulation analysis of the third-order mode shapes for different mass positions. (a) Position 1. (b) Position 2. (c) Position 3.

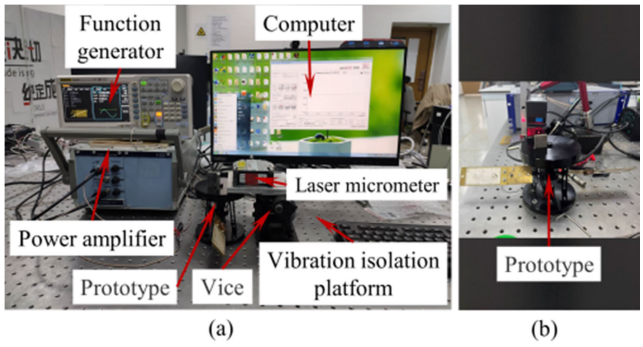

FIGURE 7. Experimental system. (a) Experiment system configuration. (b) Prototype.

the motor with the mass block at different positions is performed near the resonant frequency regions, and the optimal drive frequencies are found for the mass block at different positions.

B. EXPERIMENT ANALYSIS OF VARIABLE-NATURAL-FREQUENCY UINT AND MOTOR

As the resonant frequencies of the variable-mode piezoelectric wafer vibration response unit and the variable-natural-frequency motor have the impact on the output characteristics,

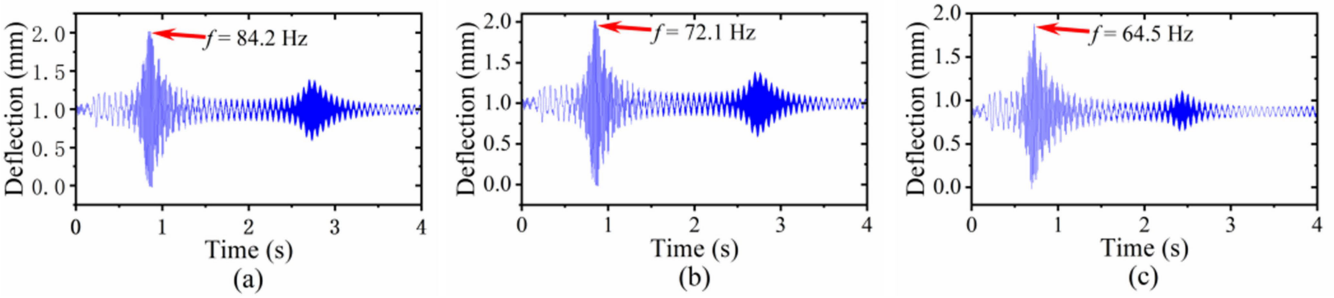

FIGURE 8. Sweep frequency analysis of variable-natural-frequency vibration response unit. (a) Position 1. (b) Position 2. (c) Position 3.

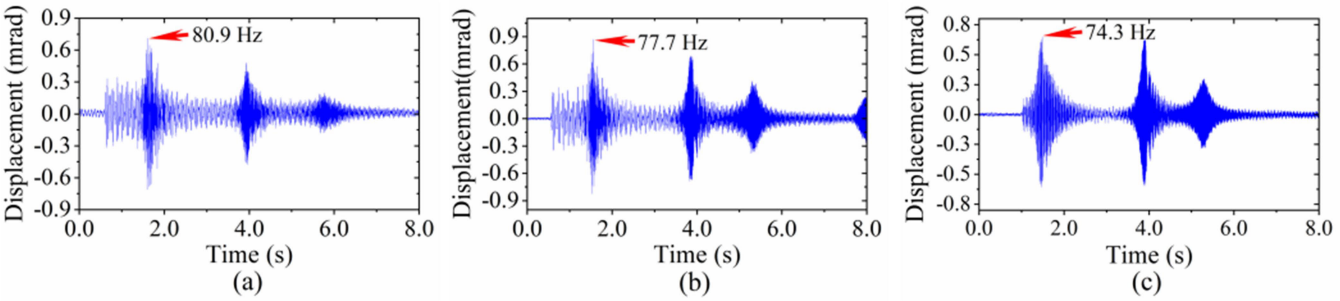

FIGURE 9. Sweep frequency analysis of variable-natural-frequency motor. (a) Position 1. (b) Position 2. (c) Position 3.

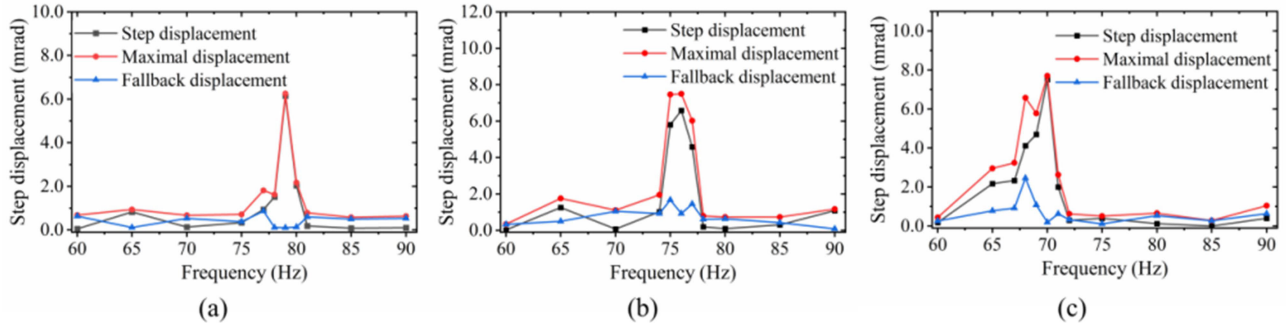

FIGURE 10. Step displacement of variable-natural-frequency motor under different frequencies. (a) Position 1. (b) Position 2. (c) Position 3.

the sweep experiments are firstly performed to evaluate the variable natural frequencies of the unit and the motor. The sweep range is 0-400 Hz, and the sweep voltage is 10 V. From Fig. 8, the natural frequencies of the variable-mode piezoelectric wafer vibration response unit with the mass block at different positions are observed in the sweep results. The resonant frequencies of the variable-mode piezoelectric wafer vibration response unit with the mass block at different positions are 84.2, 72.1, 64.5 Hz.

The sweep frequency experiments are also performed for the variable-natural-frequency piezoelectric motor and the sweep results are shown in Fig. 9. The resonant frequencies of the motor with the mass block at different positions are 80.9, 77.7, 74.3 Hz. Since the driving performance of the motor is lower in the non-resonant frequency range, the following experiments about the driving performance are conducted near the resonant frequency range.

The piezoelectric motor is further analyzed by fixing the mass block at position 1-3 with the fixed excitation voltage of 200 V, and a frequency analysis is performed according to the experiments. It can be seen in Figs. 10 and 11 that the resonant frequency of the motor is obviously different when the mass block is fixed at different positions of the single-row-hole variable-frequency substrate. The resonant frequencies are 79, 76, 70 Hz at positions 1, 2 and 3, respectively, indicating that the adjusting method of the resonant frequency of the motor by the mass block position on the single-hole variable frequency substrate is effective. The rotation speed of the motor prototype is shown in Fig. 12. The speed can be adjusted by the different positions of the mass block. The experimental rotation speed of the variable-frequency

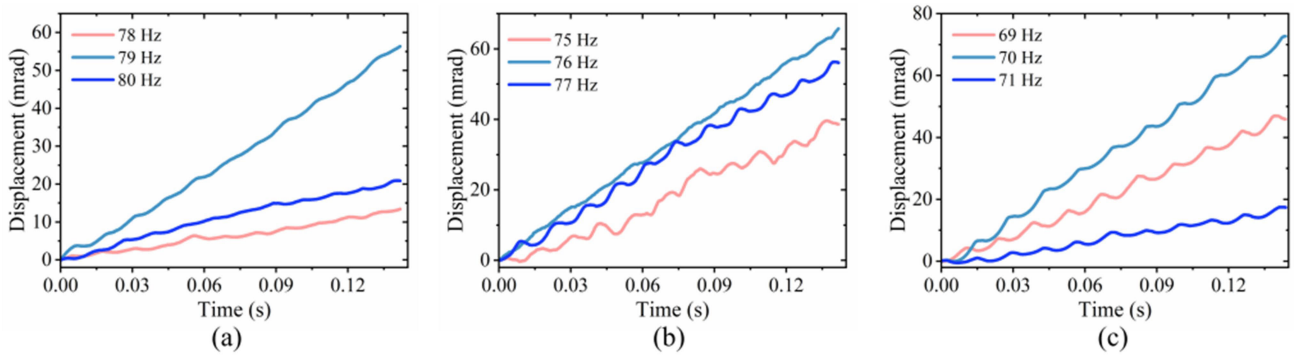

FIGURE 11. Angular displacement of variable-natural-frequency motor under different frequencies. (a) Position 1. (b) Position 2. (c) Position 3.

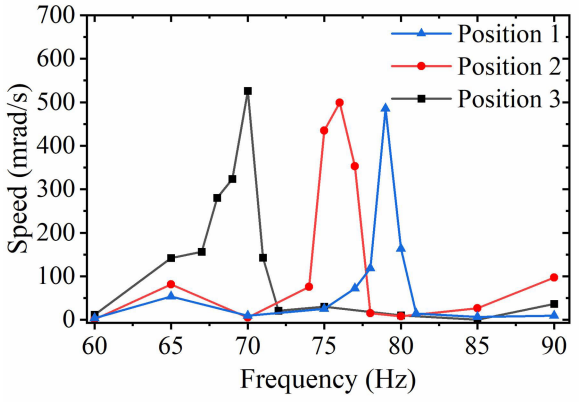

FIGURE 12. Rotation speed of variable-natural-frequency motor under different positions.

motor prototype is the maximum at position 3, which is 520 mrad/s.

The position accuracy and output torque of the motor are evaluated in the experiment. The mass block is placed at position 3 with the frequency of 1 Hz. The displacement under different voltages is shown in Fig. 13. The accuracy of the motor is 8.7 urad when the voltage is 15 V. The output torque 1.65 Nmm of the motor is evaluated under the frequency of 70 Hz, and voltage of 150 V.

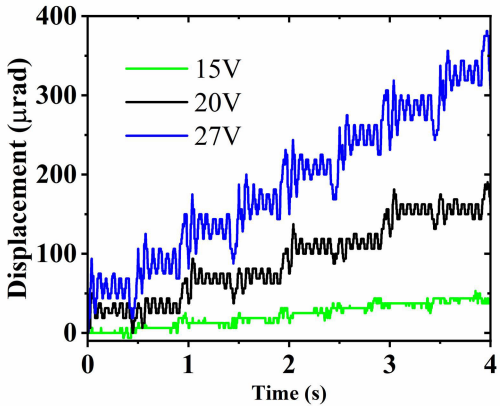

FIGURE 13. Rotation displacement of variable-natural-frequency motor.

The comparisons of the actuation method with other piezoelectric motors are shown in Table 1. The performances of the actuators, such as the accuracy, the operating frequency, the maximum speed, and the variable natural frequency are mainly compared to show the improvement of the actuation method. It can be seen that the motor has advantages as follows. The proposed motor has relatively higher accuracy. The proposed motor is driven by a low-frequency signal, which reduces noise and friction to extend service life. The proposed motor takes the ability to adjust the natural frequency, which improves the driving ability and avoids resonance.

TABLE 1. Comparison with Other Piezoelectric Motors.

Motor	Accuracy	Operating Frequency	Maximum Speed	Variable Natural Frequency
[28]	1.3 mrad	388 Hz	2.26 rad/s	No
[29]	12 mrad	161 Hz	3.23 rad/s	No
[30]	72 μrad	23.9 kHz	25.7 rad/s	No
[31]	16.4 mrad	150 Hz	2.4 rad/s	No
This work	8.7 μrad	70 Hz	520 mrad/s	Yes

V. CONCLUSION

In summary, the paper proposes, designs, manufactures and tests a low-frequency piezoelectric motor that can be used for precision positioning, precision machining, and precision measurement. First, the simulations of the piezoelectric motor structure are conducted to initially verify the feasibility of the presented piezoelectric motor motion and natural-frequency conversion. Then the structural design of the piezoelectric motor and a drive principle available for the piezoelectric motor are investigated. Moreover, the sweep frequency analysis of variable-natural-frequency motor is performed to verify the frequency characteristics. Finally, the rotation motion experiments are conducted to evaluate the performance of the piezoelectric motor. The maximum rotation speed of the designed motor is

520 mrad/s, which indicates the feasibility and validity of the variable-natural-frequency motor. In the future, we will improve the structure of the actuator to further enhance its overall performance and reduce its size. The adjustable natural-frequency motor has the application potentials and prospects for the assembly of precision electronic components, micro robots, and optical instrument precision positioning and measurement, etc.

REFERENCES

[1] N. Roshandel, D. Soleymanzadeh, H. Ghafarirad, and A. M. S. Koupaei, "A modified sensorless position estimation approach for piezoelectric bending actuators," *Mech. Syst. Signal Process.*, vol. 149, Feb. 2021, Art. no. 107231.

[2] N. Chen and X. Liu, "Dynamic modeling and attitude decoupling control for a 3-DOF flexible piezoelectric nano-positioning stage based on ADRC," *Micromachines*, vol. 13, no. 10, p. 1591, Sep. 2022.

[3] M. Meschino, L. Wang, H. Xu, R. Moradi-Dastjerdi, and K. Behdinan, "Low-frequency nanocomposite piezoelectric energy harvester with embedded zinc oxide nanowires," *Polym. Compos.*, vol. 42, no. 9, pp. 4573–4585, Jun. 2021.

[4] C. T. Chen, W. J. Su, W. J. Wu, D. Vasic, and F. Costa, "Magnetic plucked meso-scale piezoelectric energy harvester for low-frequency rotational motion," *Smart Mater. Struct.*, vol. 30, no. 10, Oct. 2021, Art. no. 105014.

[5] M. Li, J. Zhou, and X. Jing, "Improving low-frequency piezoelectric energy harvesting performance with novel X-structured harvesters," *Nonlinear Dyn.*, vol. 94, no. 2, pp. 1409–1428, Jun. 2018.

[6] H. Elahi, K. Munir, M. Eugeni, M. Abrar, A. Khan, A. Arshad, and P. Gaudenzi, "A review on applications of piezoelectric materials in aerospace industry," *Integr. Ferroelectr.*, vol. 211, no. 1, pp. 25–44, Oct. 2020.

[7] X. Chu, L. Ma, S. Yuan, M. Li, and L. Li, "Two-dimensional optical scanning of a piezoelectric cantilever actuator," *J. Electroceram.*, vol. 21, nos. 1–4, pp. 774–777, Dec. 2008.

[8] F. Filhol, E. Defaÿ, C. Divoux, C. Zinck, and M.-T. Delaye, "Resonant micro-mirror excited by a thin-film piezoelectric actuator for fast optical beam scanning," *Sens. Actuators A, Phys.*, vols. 123–124, pp. 483–489, Sep. 2005.

[9] K. H. Gilchrist, R. P. McNabb, J. A. Izatt, and S. Grego, "Piezoelectric scanning mirrors for endoscopic optical coherence tomography," *J. Micromech. Microeng.*, vol. 19, no. 9, Aug. 2009, Art. no. 095012.

[10] A. Zaszczyńska, A. Gradys, and P. Sajkiewicz, "Progress in the applications of smart piezoelectric materials for medical devices," *Polymers*, vol. 12, no. 11, p. 2754, Nov. 2020.

[11] E. Timmermann, R. Bansemer, T. Gerling, V. Hahn, K.-D. Weltmann, S. Nettesheim, and M. Puff, "Piezoelectric-driven plasma pen with multiple nozzles used as a medical device: Risk estimation and antimicrobial efficacy," *J. Phys. D, Appl. Phys.*, vol. 54, no. 2, Oct. 2020, Art. no. 025201.

[12] S. Adrar, M. El Gibari, P. Saillant, J.-C. Thomas, and R. Seveno, "Development of flexible piezoelectric sole with wireless communication for medical application," *Biomed. Signal Process. Control*, vol. 85, Aug. 2023, Art. no. 104878.

[13] R. Liu, X. Li, D. Yu, T. Cao, J. Cao, B. Wang, and D. Wu, "A 3D printed sandwich-type piezoelectric motor with a surface texture," *Rev. Sci. Instrum.*, vol. 93, no. 10, Oct. 2022, Art. no. 105003.

[14] R. Ryndzionek and Ł. Sienkiewicz, "A review of recent advances in the single- and multi-degree-of-freedom ultrasonic piezoelectric motors," *Ultrasonics*, vol. 116, Sep. 2021, Art. no. 106471.

[15] J. Wu, L. Wang, F. Du, G. Zhang, J. Niu, X. Rong, R. Song, H. Dong, J. Zhao, and Y. Li, "A two-DOF linear ultrasonic motor utilizing the actuating approach of longitudinal-traveling-wave/bending-standing-wave hybrid excitation," *Int. J. Mech. Sci.*, vol. 248, Jun. 2023, Art. no. 108223.

[16] S. Mukhopadhyay, J. Kumar, and B. Behera, "Low-operating voltage-based piezoelectric ultrasonic actuator for tactile system applications," *Ferroelectrics*, vol. 585, no. 1, pp. 163–177, Dec. 2021.

[17] V. Jūnas, G. Kazokaitis, and D. Mažeika, "Design of unimorph type 3DOF ultrasonic motor," *Appl. Sci.*, vol. 10, no. 16, p. 5605, Aug. 2020.

[18] S. Borodinas, P. Vasiljev, D. Mazeika, R. Bareikis, and Y. Yang, "Design optimization of double ring rotary type ultrasonic motor," *Sens. Actuators A, Phys.*, vol. 293, pp. 160–166, Jul. 2019.

[19] R. Bansevicius, J. Janutenaite-Bogdaniene, V. Jurenas, G. Kulvietis, D. Mazeika, and A. Drukteiniene, "Single cylinder-type piezoelectric actuator with two active kinematic pairs," *Micromachines*, vol. 9, no. 11, p. 597, Nov. 2018.

[20] S. Zhang, Y. Liu, J. Deng, X. Tian, and X. Gao, "Development of a two-DOF inertial rotary motor using a piezoelectric actuator constructed on four bimorphs," *Mech. Syst. Signal Process.*, vol. 149, Feb. 2021, Art. no. 107213.

[21] Y. Wang, Z. Xu, and H. Huang, "A novel stick-slip piezoelectric rotary actuator designed by employing a centrosymmetric flexure Hinge mechanism," *Smart Mater. Struct.*, vol. 29, no. 12, Dec. 2020, Art. no. 125006.

[22] J. Wang, H. Huang, S. Zhang, F. Qin, Z. Wang, T. Liang, and H. Zhao, "Development and analysis of a stick-slip rotary piezoelectric positioner achieving high velocity with compact structure," *Mech. Syst. Signal Process.*, vol. 145, Nov. 2020, Art. no. 106895.

[23] K. Liang, C. Li, Y. Tong, J. Fang, W. Zhong, and X. Fu, "Output characteristics and experiments of a novel low frequency rotary piezoelectric motor," *J. Mech. Sci. Technol.*, vol. 36, no. 3, pp. 1145–1156, Mar. 2022.

[24] J. Xing and Y. Qin, "A novel low-frequency piezoelectric motor modulated by an electromagnetic field," *Actuators*, vol. 9, no. 3, p. 85, Sep. 2020.

[25] J. Wang, Y. Wu, Z. Yang, X. Zhao, X. Chen, and D. Zhao, "Design and experimental performance of a low-frequency piezoelectric motor based on inertia drive," *Sens. Actuators A, Phys.*, vol. 304, Apr. 2020, Art. no. 111854.

[26] S. Zhang, J. Liu, J. Deng, and Y. Liu, "Development of a novel two-DOF pointing mechanism using a bending–bending hybrid piezoelectric actuator," *IEEE Trans. Ind. Electron.*, vol. 66, no. 10, pp. 7861–7872, Oct. 2019.

[27] S. S. Rao, *Mechanical Vibrations*, 5th ed. Prentice-Hall, 2011.

[28] L. He, G. Gao, Y. Kan, S. Hao, X. Li, X. Ge, J. Chen, and W. Chang, "Resonant-type inertial impact piezoelectric motor based on a cam locking mechanism," *Rev. Sci. Instrum.*, vol. 92, no. 7, pp. 1–12, Jul. 2021.

[29] L. He, H. Dou, X. Ge, X. Li, and G. Gao, "Resonant-type rotating piezoelectric motor with inchworm–inertia composite impact," *Rev. Sci. Instrum.*, vol. 93, no. 3, Mar. 2022, Art. no. 035004.

[30] Z. Geng, X. Li, R. Liu, Z. Wen, B. Wang, and D. Wu, "Development of a stator-rotor integrated piezoelectric actuator for precise joint rotation of the robotic arm," *Precis. Eng.*, vol. 82, pp. 360–369, Jul. 2023.

[31] L. He, Z. Wan, K. Li, Y. Wang, X. Li, X. Ge, H. Dou, Z. Shan, X. Yue, and A. Qian, "A resonant inertial impact rotary piezoelectric motor based on a self-clamping structure," *Rev. Sci. Instrum.*, vol. 94, no. 4, Apr. 2023, Art. no. 045003.

XIAOTAO LI was born in Changchun, Jilin, China, in 1980. She received the B.E., M.E., and Ph.D. degrees in mechanical engineering from Jilin University, Jilin, in 2003, 2006, and 2010, respectively.

She is currently a Professor with Jilin University. Her research interests include piezoelectric precision actuation and vision-based measurement.

SHENGJIANG WANG was born in Shangqiu, Henan, China, in 1997. He received the B.E. degree in mechanical engineering from the Henan University of Science and Technology, Henan, in 2020. He is currently pursuing the M.E. degree with Jilin University.

His research interest includes piezoelectric precision actuation.

XIANGYOU PENG was born in Zhaotong, Yunnan, China, in 1998. He received the B.E. degree from the College of Mechanical and Electrical Engineering, Soochow University, Jiangsu, China, in 2022. He is currently pursuing the M.E. degree with Jilin University.

His research interest includes piezoelectric precision actuation.

GUAN XU (Member, IEEE) was born in Changchun, Jilin, China, in 1981. He received the Ph.D. degree in vehicle operation engineering from Jilin University, Jilin, in 2009. He is currently a Professor with Jilin University. His research interests include piezoelectric precision actuation, vision reconstruction in vehicle inspection, and navigation techniques.

JINGSHI DONG was born in Jilin, China, in 1973. He received the Ph.D. degree in mechanical engineering from the School of Mechanical Science and Engineering, Jilin University, Changchun, China, in 2012.

He is currently a Professor with Jilin University. His current research interests include piezoelectric actuators, intelligent machinery and precision machinery, and in-situ tests.

FENGJUN TIAN was born in Tonghua, Jilin, China, in 1972. He received the Ph.D. degree in mechanical engineering from Jilin University, Jilin. His research interest includes piezoelectric precision actuation.